Let us now consider the criterion

$$\int_{t_0}^{t} (y_p - C\hat{x})^T Q_1 (y_p - C\hat{x})\, d\tau \quad . \quad . \quad . \quad (21)$$

associated with eqn. 17. It is a special case of the above problem, if we assume $v \equiv 0$, i.e. $Q_2 \infty$ and $Q_3 = 0$; $Q_2 \infty$ means that Q_2 is a diagonal matrix with arbitrary large entries. The solution of eqns. 21 and 17 is thus

$$\dot{\hat{x}} = A\hat{x} + Bu + M(t)\, Q_1 (y_p - C\hat{x}) \quad . \quad . \quad . \quad (22)$$

$$\dot{M} = MA^T + AM - MC^T Q_1 CM \quad . \quad . \quad . \quad (23)$$

$$M(t_0) = \infty \quad . \quad . \quad . \quad (24)$$

Setting $LM = ML = I$ (identity matrix), eqns. 23 and 24 are converted into

$$\dot{L} = -A^T LLA + C^T Q_1 C \quad . \quad . \quad . \quad (25)$$

$$L(t_0) = 0 \quad . \quad . \quad . \quad (26)$$

Now, if we observe that the gain of our initial problem (eqns. 1 and 3) is constant because of the constant optimisation period T_1, this gain is obtained by integrating eqn. 25 from $-T_1$ to 0. This yields eqns. 4, 5 and 6. Eqn. 7 is the well known solution of eqn. 5.

Regulator: Although the optimal controller solution can be immediately written by duality, we work it out as above. We first consider the problem of finding $u(t)$ that minimises

$$\int_{0}^{T_1} u^T Ru\, d\tau \quad . \quad . \quad . \quad (27)$$

associated with

$$x(T_1) = 0 \quad . \quad . \quad . \quad (28)$$

and

$$\dot{x} = Ax + Bu \quad . \quad . \quad . \quad (29)$$

This is a special case of the optimal linear quadratic control problem, whose performance index is

$$\tfrac{1}{2} x^T(T_1)\, Fx(t_1) + \tfrac{1}{2}\int_{0}^{T_1} (x^T Qx + u^T Ru)\, d\tau \quad . \quad . \quad . \quad (30)$$

Eqns. 27 and 28 are deduced from eqn. 30, putting $F\infty$ and $Q = 0$. So the solution of eqns. 27, 28 and 29 is

$$u^*(t) = -R^{-1} B^T K(t)\, x(t) \quad . \quad . \quad . \quad (31)$$

where

$$-\dot{K} = KA + A^T K - KBR^{-1} B^T K \quad . \quad . \quad . \quad (32)$$

$$K(T_1) = \infty \quad . \quad . \quad . \quad (33)$$

Setting $MK = KM = I$, eqns. 32 and 33 become

$$\dot{M} = AM + MA^T - BR^{-1} B^T \quad . \quad . \quad . \quad (34)$$

$$M(T_1) = 0 \quad . \quad . \quad . \quad (35)$$

The receding-horizon optimal control is now straightforward: (c.f. eqns. 11, 12 and 13). At any time, the control law is that of eqn. 31 replacing $K(t)$ by $K(0)$, since the optimisation period is constant (T_1). Complete controllability, and complete observability for the estimator problem, is necessary to guarantee the asymptotic stability of the closed loop, as shown in a paper by Kleinman.[4]

Conclusion: Filter and control algorithms that have physical meanings and a limited number of coefficients to be chosen *a priori* have been described. Moreover, the computations are concerned with linear equations, instead of the classical Riccati equation. Complete derivations and discrete versions can be found in Reference 3.

Y. A. THOMAS

Laboratoire d'Automatique
École Nationale Supérieure de Mécanique
3 Rue du Maréchal Joffre
44041 Nantes, France

9th December 1974

References

1 DE LARMINAT, P.: 'Filtrage et commande selon un critère à horizon mobile', *Rev. Rairo*, May 1972, pp. 73–86
2 DE LARMINAT, P., SARLAT, D., and THOMAS, Y.: 'Invariant imbedding and filtering: a moving horizon criterion', *JACC*, June 1974 (Austin)
3 THOMAS, Y., and BARRAUD, A.: 'Commande optimale à horizon fuyant', *Rev Rairo*, April 1974
4 KLEINMAN, D. L.: 'An easy way to stabilize a linear constant system', *IEEE Trans.*, 1970, AC-15, p. 692

SUBNANOSECOND-PULSE GENERATOR WITH VARIABLE PULSEWIDTH USING AVALANCHE TRANSISTORS

Indexing term: Bipolar transistors, Pulse generators

The letter describes a pulse generator with epitaxial silicon planar transistors working in the avalanche-breakdown mode. The risetime is 150 ps and the fall time 200 ps. The pulsewidth can be varied continuously between 0·3 and 120 ns, without changing the maximum amplitude of about 15 V. Simple rules for the exact design of the circuitry are given.

Avalanche transistors are excellently suited for the generation of pulses with high power and steep edges, which are needed in subnanosecond-measurement techniques. Similar to pulse generators with mercury relays, normally an originally charged delay line is used, which is discharged through a load resistor R_L when the transistor is fired by a positive trigger pulse v_{tr} (Fig. 1A).[1-3] During turn-on, the transistor switches from a stable operating point with high collector-emitter voltage ($v_{CE} = V_I \simeq BV_{CBO}$*) and very small collector current to a monostable operating point with lower voltage ($v_{CE} = V_{II} < BV_{CEO}$†), high current and a very small differential resistance.[4] If the load resistance R_L equals the impedance Z of the delay line, the amplitude of the positive output pulse is

$$\Delta V_L = \tfrac{1}{2}(V_I - V_{II}) \quad . \quad . \quad . \quad (1)$$

The pulsewidth is twice the delay time t_0 of the line because the transistor is turned off by the pulse that has been reflected at the open end of the line.

The method described has the disadvantages that the pulsewidth is fixed by the length of the line and that the falling edge is normally strongly distorted (Fig. 1B). The last fact is particularly disturbing if a small pulsewidth is desired. These disadvantages can be avoided if the avalanche transistor T_1 is not turned off by the reflected pulse, but by an additional pulse generated by a second avalanche transistor T_2 at the end of the delay line (Fig. 2A). The purpose of the line between C_1 and C_2 is now the decoupling of the two transistors for a certain range of time.‡

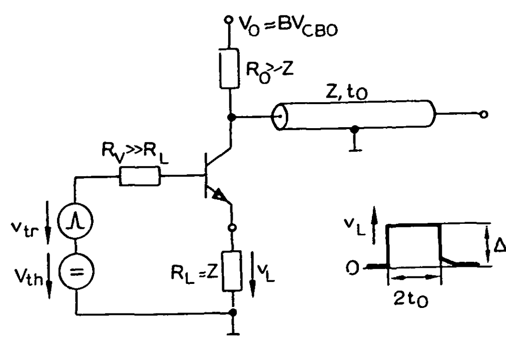

Fig. 1A *Usual pulse generator with one avalanche transistor*

* BV_{CBO} = collector–base breakdown voltage (open emitter)

† BV_{CEO} = collector–emitter breakdown voltage (open base) for medium currents

‡ In Reference 2, a diode and capacitors are used for decoupling. This method has the disadvantages that the top of the pulse is inclined and the turnoff time increases

The width t_P of the output pulse is determined by the phase relationship of the trigger pulses at the two bases of T_1 and T_2. The phase difference can be varied continuously by the monostable multivibrator m.m.$_2$. Triggering T_1 at the time t_1 and T_2 at t_2, we obtain

$$t_P = t_0 + t_2 - t_1 \quad . \quad . \quad . \quad . \quad . \quad . \quad . \quad . \quad . \quad . \quad (2)$$

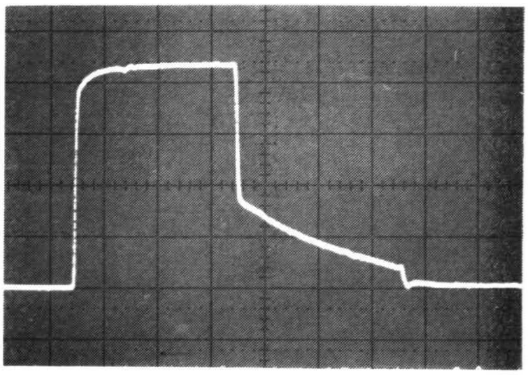

Fig. 1B *Output voltage v_L of pulse generator of Fig. 1A*
Horizontal: 5 ns/division; vertical: 5 V/division

with

$$0 < t_P < 2t_0$$

t_0 is the delay time of the line. The pulsewidth reaches its maximum value ($t_{P,max} \simeq 2t_0$) if T_2 is triggered immediately before the pulse, which has been generated by T_1, reaches the collector C_2 and is reflected there. The height ΔV_{C2} (< 0) of the pulse generated by T_2 has to be sufficiently large that it brings the voltage at C_1 exactly down to zero. The output voltage v_L also jumps back to zero because the transistor T_1 goes into saturation. The condition for that has been derived in Reference 4:

$$\Delta V_{C2} = -V_I/2 \quad . \quad . \quad . \quad . \quad . \quad . \quad . \quad . \quad . \quad . \quad (3)$$

With

$$\Delta V_{C2} = -\frac{Z}{Z+R_{E2}}(V_I - V_{II}) \quad . \quad . \quad . \quad . \quad . \quad (4)$$

we obtain, for the d.c. emitter resistance of T_2,

$$R_{E2} = Z(1-2V_{II}/V_I) \quad . \quad . \quad . \quad . \quad . \quad . \quad . \quad . \quad (5)$$

To avoid reflections at C_1 and C_2, which may§ distort the

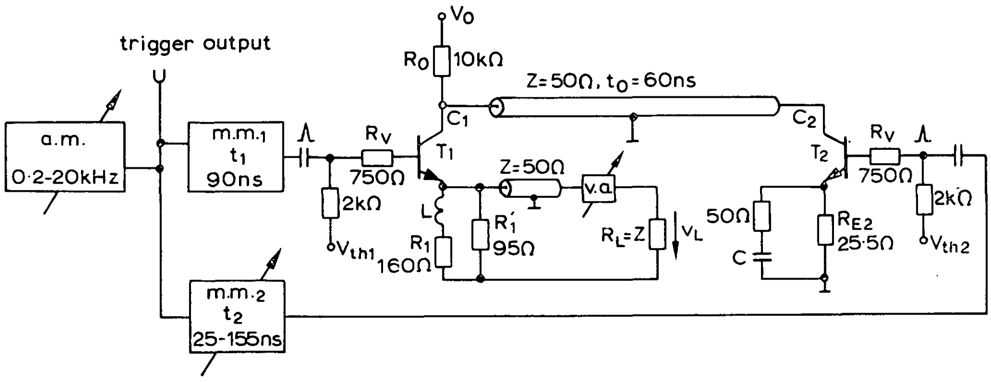

Fig. 2A *Circuit diagram of pulse generator with improved pulse shape and variable pulse width*
L = 220 nH, C = 20 pF).
A.M.: astable multivibrator, M.M.: monostable multivibrator, V.A.: variable attenuator

output voltage, the d.c. emitter resistance of T_1 must be[4]

$$R_{E1} \simeq R_{E2} \quad . \quad . \quad . \quad . \quad . \quad . \quad . \quad . \quad . \quad . \quad . \quad (6)$$

with R_{E2} from eqn. 5 and (Fig. 2A)

$$\frac{1}{R_{E1}} = \frac{1}{R_1} + \frac{1}{R_1'} + \frac{1}{R_L} \quad . \quad . \quad . \quad . \quad . \quad (7)$$

The output voltage swing becomes now smaller than in eqn. 1:

$$\Delta V_L = \frac{V_I}{2} - V_{II} \quad . \quad . \quad . \quad . \quad . \quad . \quad . \quad . \quad . \quad (8)$$

Both transistors used in this pulse generator have the voltages

$$V_I \simeq V_{CBO} = 60\,\mathrm{V} \quad \text{and} \quad V_{II} = 15\,\mathrm{V}$$

Inserting these values in eqn. 5, we have $R_{E2} = 25\,\Omega$. The measured optimal value ($R_{E2} = 25{\cdot}5\,\Omega$) used in Fig. 2A is only 2% higher. The small difference results from the fact that the base currents of both transistors are neglected in the derivation of eqns. 3–6 ($R_V \gg R_{E1}, R_{E2}$)

Additional elements have been used to improve the pulse shape. The RL series connection‖ parallel to R_L and the RC series connection parallel to R_{E2} avoid small creeping effects at the end of the rising slope (Fig. 1B) and the falling slope of the output pulse. Rules for the quantitative design have been derived in Reference 4.

Figs. 2B(i) and 2B(ii) show the shape of the positive output pulse for two different pulsewidths. There is a distinct improvement compared with the pulse shape in Fig. 1B. Using a simple mounting technique, a risetime (10 to 90%)

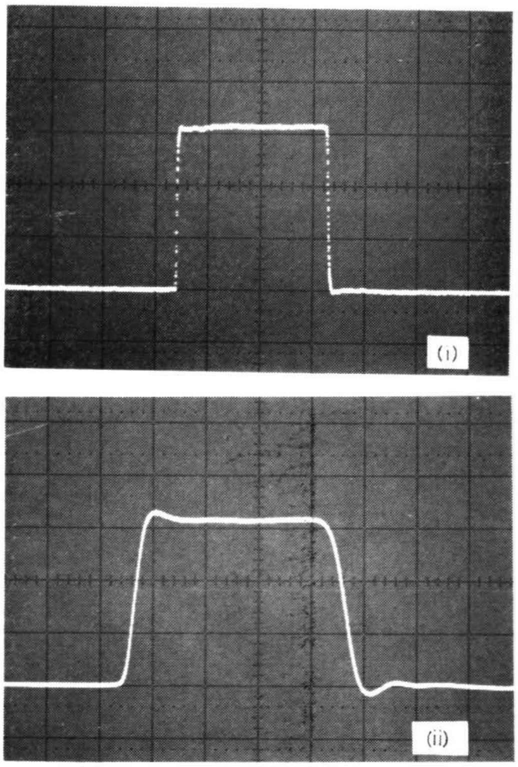

Fig. 2B *Output voltage v_L of pulse generator in Fig. 2A for two different pulsewidths t_p*
(i) t_p = 30 ns (10 ns/division)
(ii) t_p = 2 ns (0·5 ns/division)
Risetime t_r = 150 ps, fall time t_f = 200 ps
The vertical unit is 5 V

§ Reflections can influence the output earliest at 2 t_0 (twice the delay time) after the rising edge of the output pulse

‖ For a further improvement, a somewhat more complicated network might be necessary.[4] It has been used for the generation of the pulses shown in Figs. 2B and 2C of less than 150 ps has been obtained. The fall time is slightly larger (200 ps), mainly due to the influence of the delay line. The pulsewidth (at 50% of the voltage swing) can be varied continuously from 0·3 to 120 ns, without changing the amplitude of about 15·5 V and the slopes of the pulse. Using a variable attenuator, the amplitude can be varied and, with a coaxial-line transformer (not shown in Fig. 2A), it is possible to invert the pulse. The repetition frequency is adjustable by an astable multivibrator (a.m., Fig. 2A) from 0·2 to 20 kHz. We have made no effort to reach the maximum frequency, given mainly by the maximum permissible power dissipation of the transistors.

To obtain switching times, standard silicon planar transistors can be used, which, however, must have a thin, lowly doped epitaxial layer.[5] Such transistors can be identified in a simple way by measuring the output characteristics in common-base configuration (constant emitter current,) which already show a negative slope (negative differential resistance) for small currents.[6] The cutoff frequency is of little influence. The shortest risetime we could obtain with standard transistors was 100 ps. Using an improved mounting technique, even lower values are expected. The excellent properties, the simple design and the low cost make this pulse generator an useful tool for subnanosecond-pulse measurement techniques.

H.-M. REIN 10th December 1974

Ruhr-Universität Bochum
Institut für Elektronik
4630 Bochum, Postfach 2148, W. Germany

M. ZAHN ¶
Dornier System GmbH
7990 Friedrichshafen, Postfach 648, W. Germany

References

1 ZAHN, M.: 'Das Schaltverhalten eines Transistors im Lawinendurchbruch und Bau eines Impulsgenerators mit Lawinentransistoren-Diplomarbelt am Institut für Halbleitertechnik, Universität Stuttgart' 1967
2 MITCHELL, W. B.: 'Avalanche transistors give fast pulses', *Electronic Design*, 1968, **6**, pp. 202–209
3 PFEIFFER, W.: 'Ein einfacher Impulsgenerator für Reflexionsfaktor- und Sprungübertragungsmessung', *Int. Elektron. Rundsch.*, 1971, **25**, pp. 268–272
4 REIN, H.-M.: 'Erzeugung variabler Rechteckimpulse mit Lawinentransistoren', *Arch. Elektron. Übertragungstech.*, 1975, **29** (to be published)
5 REIN, H.-M.: 'Ein Beitrag zum Schaltverhalten von Epitaxial-Planartransistoren im Bereich des Lawinendurchbruchs'. Diskussionssitzung der Nachrichtentechn. Gesellschaft (NTG), Bad Reichenhall, W. Germany, 1967
6 REIN, H.-M., SCHAD, T., and ZÜHLKE, R.: 'Der Einfluss des Basisbahnwiderstandes und der Ladungsträgermultiplikation auf das Ausgangskennlinienfeld von Planartransistoren', *Solid-State Electron.*, 1972, **15**, pp. 481–500

¶ Formerly with the Institut für Halbleitertechnik, Universität Stuttgart, W. Germany

INFLUENCE OF ACTIVE-LAYER WIDTH ON THE PERFORMANCE OF HOMOJUNCTION AND SINGLE-HETEROJUNCTION GaAs LIGHT-EMITTING DIODES

Indexing terms: Light-emitting diodes, Optical-communication equipment

For epitaxial GaAs homojunction and single-heterojunction (s.h.) l.e.d.s, light power output and risetime as a function of active-layer width were investigated. Narrow-base homojunction diodes can be markedly faster than s.h. diodes, the rise time of which is limited by the electron lifetime. However, for equal width of the active layer and equal injection level, the light power output of s.h. diodes is superior, compared with that of homojunction diodes.

There is considerable interest in powerful and fast incoherent l.e.d.s as light generators for communication systems using optical fibres. Only recently, a 100 Mbit s^{-1} fibre-optic communication system employing a GaAs l.e.d. has been reported.[1] Because of high internal quantum efficiency and low fibre loss at the emitted wavelength, GaAs material for l.e.d.s is advantageous. Although investigations have been made on GaAs l.e.d.s on risetime and light power output,[2,3] no systematic work on the influence of relevant technological parameters on the performance of l.e.d.s exists. Hence risetime and light power output as a function of active-layer thickness were studied for two types of GaAs diodes: epitaxial homojunction and single-heterojunction l.e.d.s. The diodes were fabricated from l.p.e. layers grown in this laboratory. A schematic cross-sectional view of a homojunction l.e.d. is shown in Fig. 1*a*. On an *n* substrate, an *n* GaAs layer (layer 1, Sn doped, $n = 8 \times 10^{17}$ cm^{-3}, $d_1 = 2{\cdot}5$ µm) and a *p* GaAs layer (layer 2, Ge doped, $p = 1 \times 10^{18}$ cm^{-3}) were grown. The thickness d_2 of the active layer 2 was varied in the range $d_2 = w = 0{\cdot}7$–10 µm.

For the s.h. diodes, a 4-layer structure was grown (cross-sectional view in Fig. 2*a*). Beginning from the *n* substrate, the four layers had the following specifications:

Layer 1: *n* GaAs, Sn doped, $n = 8 \times 10^{17}$ cm^{-3}, $d_1 = 2{\cdot}5$ µm

Layer 2: *p* GaAs, Ge doped, $p = 1 \times 10^{18}$ cm^{-3}

Layer 3: *p* $Ga_{0\cdot6}Al_{0\cdot4}As$, Ge doped, $p = 1 \times 10^{18}$, $d_3 = 0{\cdot}8$ µm

Layer 4: *p* GaAs, Ge doped, $p = 1 \times 10^{18}$, $d_4 = 0{\cdot}8$ µm

The layer thickness d_2 was varied between $d_2 = w = 0{\cdot}6$ and 7 µm. Layer 4 was incorporated for contacting purposes only.

Both types of diode had the same geometry; they were mesa etched, with a diameter of 150 µm for the light-emitting area and of 260 µm for the junction area. The diodes were mounted with the substrate on the heatsink of conventional microwave packages (without cover). The l.e.d.s were mounted on an optical bench, and the emitted light was focused with two lenses on the active area of a Si avalanche photodiode. The diodes were operated with 300 mA rectangular current pulses of 300 ns duration (50Ω source). The risetime of the entire measuring setup was below 1 ns (checked by laser experiments). Risetimes were measured between 0 and 80% of maximum light output. Delay times were not considered.

For narrow-base homojunction l.e.d.s, that is, when w is smaller than the electron diffusion length L, the light output P and risetime τ_r increase almost linearly with w (Fig. 1*b*).

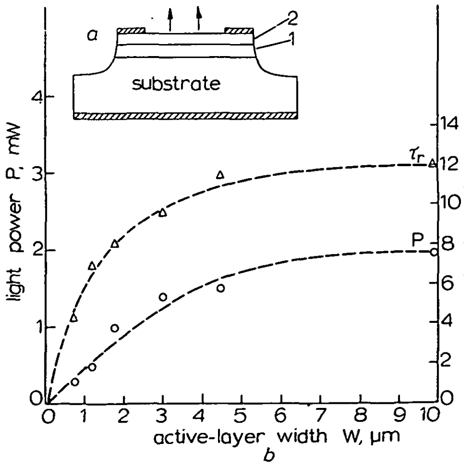

Fig. 1
a Cross-sectional view of homojunction l.e.d.
b Light power P and risetime τ_r against active-layer width

Under this condition, and at constant injection level, the number of minority carriers in the light-emitting volume, and hence P, increases with increasing w. As a consequence, the charging of the diffusion capacitance takes more time and τ_r rises also. However, for $w > L$, the number of carriers, and therefore generated photons, becomes constant. As a result, light output and risetime saturate. A diffusion length of $L = 7$ µm, which has been reported for the given doping level,[4] is in agreement with our measurements. In Fig. 2*b*, P and τ_r as functions of active width w are plotted for s.h. l.e.d.s. P exhibits a broad maximum near $w = 2$ µm ($P_{max} = 3{\cdot}7$ mW). The slight decrease in P for $w > 2$ µm is due to